Influence of Jordanian zeolite on the performance of a solar still: experiments and CFD simulation studies

Yazan Taamneh

ABSTRACT

Computational fluid dynamics (CFD) simulations were performed for experiments carried out with two identical pyramid-shaped solar stills. One was filled with Jordanian zeolite-seawater and the second was filled with seawater only. This work is focused on CFD analysis validation with experimental data conducted using a model of phase change interaction (evaporation-condensation model) inside the solar still. A volume-of-fluid (VOF) model was used to simulate the inter phase change through evaporation-condensation between zeolite-water and water vapor inside the two solar stills. The effect of the volume fraction of the zeolite particles ($0 \leq \phi \leq 0.05$) on the heat and distillate yield inside the solar still was investigated. Based on the CFD simulation results, the hourly quantity of freshwater showed a good agreement with the corresponding experimental data. The present study has established the utility of using the VOF two phase flow model to provide a reasonable solution to the complicated inter phase mass transfer in a solar still.

Key words | CFD simulation, Jordanian zeolite, solar still, VOF model

Yazan Taamneh
Department of Aeronautical Engineering,
Jordan University of Science and Technology,
PO Box 3030,
Irbid 22110,
Jordan
E-mail: *ymtaamneh@just.edu.jo*

INTRODUCTION

The drastic increase in demand for safe drinking water is growing continuously in developing countries. Inadequate access to fresh water resources is the cause of major health issues nowadays. In recent decades, Jordan has received insufficient rainfall which has led to an increase in water salinity, although it has huge solar potential in most regions. Therefore, the use of small scale solar distillation units is appropriate. Desalination is a very old technology with a long history. It first appeared in 1872 when a still at Las Salinas on the northern deserts of Chile provided a mining community with potable water (Tiwari *et al.* 1997; Hamdan *et al.* 1999; Taamneh & Taamneh 2012).

A solar still is merely an air tight basin with a sloping top cover of a transparent material (usually glass) that utilizes the solar radiation to produce fresh water. Solar energy is available on site, free and can reduce fuel consumption and pollution. (Malik *et al.* 1982; Khanna *et al.* 2008; Kabeel *et al.* 2014).

A number of experimental and theoretical studies are being executed, to find a better design to improve the performance of solar stills. Three different types of solar still were experimentally investigated by (Tiwari *et al.* 1986; 2003). They understood that a single slope solar still has a higher performance than a double slope in winter. In summer, the performance of a double slope is better. The productivity of a solar still was enhanced by using it as a solar collector for exterior heating of water (Voropoulos *et al.* 2001). Running cool water over the glass cover was proposed by Esfahani *et al.* (2011) in a portable solar still to improve its performance.

The effect of air blowing inside the solar still was investigated experimentally by many researchers (Tiwari *et al.* 1997; Kumar & Tiwari 1998; Velmurugana & Srithar 2007). The air can be drawn inside the still by means of a fan. The solar still performance with air motion was estimated and compared to that without air motion. The experimental

doi: 10.2166/ws.2016.091

results showed that a considerable increase in the fresh water productivity is obtained when the air is blown inside the solar still. Taamneh & Taamneh (2012) concluded that using a fan powered by photovoltaic solar panels was effective in increasing the evaporation rate and, consequently, the condensation rate (fresh water). They showed that the productivity increased by 25 percent compared with a free convection solar still. Tiwari *et al.* (2003) showed that increasing the temperature gradient between the water and the glass surface produced more fresh water. They used for this purpose continuous water flow over the glass cover coupled with a solar collector. The same results were also obtained by Abu-Arabi *et al.* (2002). El-Sebaii *et al.* (2011) investigated the stepped solar still. They showed that water flow rate, water inlet temperature and wind speed have significant effects on the production of fresh water.

In general, the problem with experimental studies is the time and cost. Therefore, computational fluid dynamics (CFD) modeling has become an attractive tool for many researchers to find better designs of solar still. On the other hand, CFD can be used for a large number of difficult situations under different operating parameters. The governing equations in a single-slope solar still were solved using a finite-difference algorithm technique by Rheinländer (1982). He reported that the agreement between experimental and numerical mass transfer data was good. Djebedjian & Abou Rayan (2000) used a finite volume method to investigate the efficiency of solar stills. They illustrated by graphs the zones where water vapor occurred opposite circulation inside the solar still. Steady and unsteady behavior of laminar and turbulent flow in a trapezoidal solar still were investigated using CFD simulations by Papanicolaou & Belessiotis (2005). They showed that the Rayleigh number and geometry are the main parameters that governed the flow field inside the enclosure. Rahbar & Esfahani (2013) investigated the strength of CFD simulations in evaluating the hourly yield of a single-slope solar still. They proposed a new equation based on Chiltone-Colburn to evaluate the productivity of a solar still. They showed that the CFD can predict the Nu number with high accuracy compared with productivity evolution.

There seems to be a lack of interest in the CFD optimization of a solar still. Therefore, the purpose of this research is to develop a 3-dimensional two phase model for evaporation and condensation in a pyramid-shaped solar still using ANSYS FLUENT. Particular attention was paid to the inter phase change through evaporation-condensation between zeolite-water and water vapor inside the pyramid solar still with different zeolite volume fractions using a volume-of-fluid (VOF) model. In addition, the aim of this study is to estimate numerically the hourly freshwater productivity of the pyramid solar still, and compare the simulation results with experimental data under Jordanian climate conditions.

MATERIAL AND METHODS

Experimental setup

The experiments were undertaken over 3 days in June under Jordanian weather conditions. Brackish water was utilized in experiments with a salinity level in the range of 30–35 g/l. Figure 1 shows the unit that was made up of a metallic container, filled with brackish water to a certain level below the top of the basin height. The surface area of water for the pyramid solar still was 1 m × 0.95 m (Taamneh & Al-Shyyab 2016). The four identical triangles are joined together using adhesive silicon to form the pyramid structure. These triangles are wrapped around a square base container made of galvanized steel. The objective of this design is to enhance the exposed areas for condensation. The triangular glass panels are inclined at an angle of 38° in order to enhance the dropwise condensation process.

Figure 1 | Photograph of pyramid-shaped solar still.

Moreover, increasing the exposed areas increases the amount of thermal energy reaching the basin at midday. The purpose of an adhesive silicon and rubber gasket that was sited between the glass cover and the aluminum container frame was to prevent any leakage of water vapor. Holes were pierced into the container as well as through the glass to allow access of brackish water into the basin during initial loading and installing temperature thermocouples. In addition, a vent line is linked to the tee-pipe to control the water level of the brackish water.

An insulating material was wrapped around the container so that no heat was lost. The condensed water is drawn through a channel to the outlet. The fresh water was continuously collected using a plastic vessel. The base of the solar still that is made of galvanized iron of thickness 0.15 cm was coated with black paint. The solar radiation is transmitted through a 4 mm thick glass cover with transmissivity of about 0.88 and then the heat is absorbed and stored by the basin.

The thermal energy stored is transferred by conduction and convection to the brackish water. When enough heat has been absorbed by the mixture, evaporation can take place and will be subjected to phase change. The water vapor escapes from the brackish water surface, rises up and comes into contact with the glass surface. The vapor then condenses from vapor back to liquid. The fresh water then drips and drains through the inclined surface to the outlet (plastic vessel).

Zeolite-water mixture

A sample of Jordanian zeolite was collected from the Al Mafraq district. Particle-size distribution analysis of powdered zeolite was performed. The particle size distribution (PSD) of all samples was measured by means of dynamic light scattering (see Figure 2). The samples were dried at

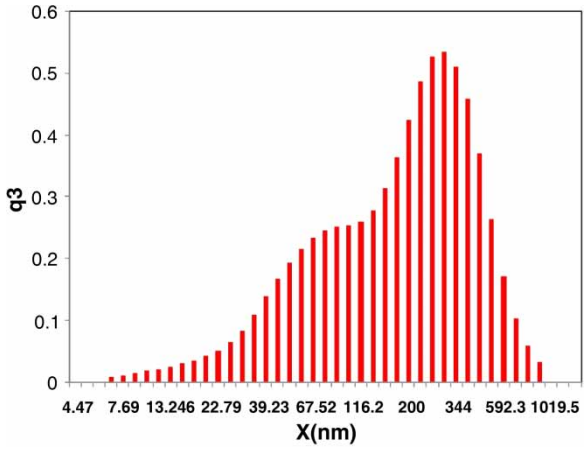

Figure 2 | Zeolite PSD.

120 °C for 12 hours. Various volume fractions of zeolite of average particle size 0.25 μm were loaded in one of the solar stills. Zeolite is one of a family of chemical compounds of aluminosilicate minerals that are capable of reversible absorption ($Na_2Al_2Si_3O_{10}{\cdot}2H_2O$) (see Table 1). The zeolite absorbs an amount of thermal energy and emits heat when it comes in contact with water. By continuous heating zeolite can store up to four times more heat than water and releases water vapor at the same time. This excess vapor rises and condenses over the glass surface which in turn increases the total amount of fresh water. In this study the zeolite-water mixture is considered as a single phase, thus, the zeolite particles and the base fluid (brackish water) are in thermal equilibrium and the relative velocity is negligible or equal to zero. Therefore, the effective thermo-physical properties mainly depend on the volume concentration of the zeolite particles as well as the properties of the base fluid. General correlations for the effective thermal conductivity, viscosity and thermal expansion coefficient of zeolite-water were

Table 1 | Physical properties of modified solar still components (0 °–100 °C)

	Thermal conductivity W/m.K	Bulk density g/cm³	Porosity %	Specific heat kJ/kg.K	Heat of absorption kJ/kg	Storage density kWh/m³
Zeolite	0.32–38	0.9–1.1	30–47	0.87–0.91	1,019–1,132	180–300
Brackish water	0.67	1.022	–	4.19	420–840	65–82
Glass	1.02	2.53	–	0.8	600–800	22–80
Absorber (aluminum)	204	2.7	–	0.89	500–900	27–70

developed in terms of the volume fraction, temperature, particle diameter and the base fluid physical properties. These correlations have been processed in FLUENT using user defined functions.

Density

The density of zeolite–water fluid is based on the physical principle of the mixture rule:

$$\rho_{eff} = (1 - \phi_p)\rho_f + \phi\rho_p \quad (1)$$

where f and p refer to the fluid and zeolite nanoparticle respectively and ϕ is the volume fraction of the nanoparticles.

Viscosity

Various models of viscosity have been employed by researchers to model the effective viscosity of nanofluids as a function of volume fraction. For low volume fraction of nanoparticles, Einstein's model can be employed to predict the viscosity of the nanofluids given as:

$$\mu_{eff} = (1 + 2.5\phi_p)\mu_f \quad (2)$$

Thermal conductivity

A kinetic model is adopted in this study to estimate effective thermal conductivity of the zeolite-water mixture. In fact, there are two types of kinetic model suggested in the literature (Khanafer *et al.* 2003). One supposes that the particles are in motion inside the base fluid and the other supposes that the particles are stationary. In this work, the stationary particle model is utilized in the CFD simulations:

$$k_{eff} = k_f\left[1 + \frac{k_p\phi r_f}{k_f(1-\phi)r_p}\right] \quad (3)$$

where r_f and r_p are the radius of the water particle (3.2×10^{-10} m) and zeolite particle (25×10^{-8} m), respectively.

Thermal expansion coefficient

The thermal expansion of the zeolite-water mixture can be evaluated employing the volume fraction of the particles on weight basis as follows:

$$\beta_{eff} = (1 - \phi_p)\beta_f + \phi_p\beta_p \quad (4)$$

Heat capacity

The specific heat of the nanofluid is formulated by assuming a thermal equilibrium between the nanoparticles and the base fluid phase as follows:

$$c_{eff} = \frac{(1 - \phi_p)\rho_f c_f + \phi_p\rho_p c_p}{\rho_{eff}} \quad (5)$$

where ρ_p is the density of the nanoparticle, ρ_f is the density of the base fluid, ρ_{eff} is the density of the zeolite-water mixture, and c_p and c_f are the heat capacities of the particle and the base fluid, respectively.

Measurements

Three thermocouples have been installed for measuring the temperature of the brackish water in the basin, the glass and the inside air. It has been found from temperature measurements that the average maximum temperature in summer was around 35 °C and the maximum solar radiation was about 1,060 W/m^2. The experiments started around 6:00 am and temperatures were recorded every 30 min for approximately 12 h. The physical properties of the modified solar still are presented in Table 1.

NUMERICAL COMPUTATIONS

Geometry and grid arrangement

The geometry and mesh were carried out using GAMBIT to generate hex-dominant finite volume elements. It is an integrated preprocessor for CFD analysis. Figure 3 shows

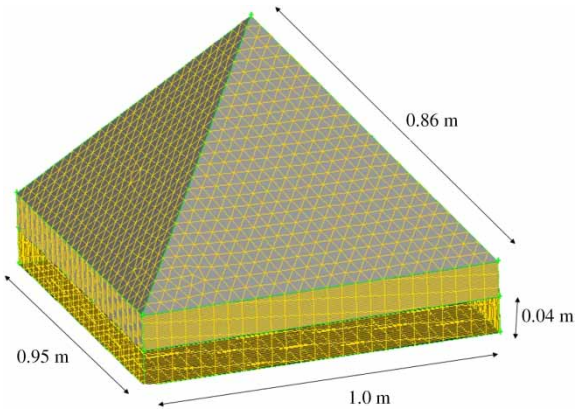

Figure 3 | Computational domain and the grid generation using Gambit.

the geometry and mesh. It shows the isometric view of the computational domain mesh that was used for this study. A total of 2.7 million cells was found to be sufficient.

Computational model

In this study, the evaporation and condensation processes were simulated using the VOF model improved by Hirt & Nichols (1981). In this work, the VOF model in a commercial CFD code FLUENT 6.2 was utilized. The VOF model can follow the interface between two phases. Thus, it has been used widely in analyzing any two phase flow system where the change of interface is significant. The governing equations can be solved using the volume fraction in each cell. The summations of volume fraction for each phase in one cell is unity.

$$\sum_{k=1}^{n} \alpha_k = 1 \tag{6}$$

The volume fraction in each cell is used to evaluate all properties in the VOF model. If the two phases are indexed by the subscripts 1 and 2 in the two-phase system, and the volume fraction of the second phase is being followed, then in each cell the density is given by:

$$\rho = \alpha_2 \rho_2 + (1 - \alpha_2)\rho_{eff} \tag{7}$$

The viscosity is calculated in the same way. Thus, all properties in each cell begin to be different based on the volume fraction. The change of the vapor interface is followed by the solution of a continuity equation for the volume fraction. For the kth phase, this equation is given by:

$$\frac{\partial \alpha_k}{\partial t} + \vec{v}\,\nabla \alpha_k = \frac{S\alpha_k}{\rho_k} \tag{8}$$

where $S\alpha_k$ is the mass source term. In evaporation and condensation processes, the mass transfer between the phases is simulated by modeling the mass source term. A single momentum equation shown in Equation (9) can be solved throughout the domain with no slip between the phases:

$$\frac{\partial}{\partial t}(\rho \vec{v}) + \nabla(\rho \vec{v}\vec{v}) = -\nabla p + \nabla\left[\mu_{eff}(\nabla \vec{v} + \nabla \vec{v}^T)\right] + \rho \vec{g} + \vec{F} \tag{9}$$

where v is treated as the average mass flux of phases:

$$v = \frac{\alpha_1 \rho_{eff} v_1 + \alpha_2 \rho_2 v_2}{\rho} \tag{10}$$

In this CFD simulation, $\vec{F}$ represents the surface tension forces at the interface. The energy equation, shown below, is also shared among the phases:

$$\frac{\partial}{\partial t}(\rho E) + \nabla(\vec{v}(\rho E + p)) = \nabla(k_{eff} \nabla T) + S_h \tag{11}$$

The energy, E, and temperature, T, are treated as mass-averaged variables in the VOF model:

$$E = \frac{\sum_{k=1}^{n} \alpha_k \rho_k E_k}{\sum_{k=1}^{n} \alpha_k \rho_k} \tag{12}$$

where E_k for each phase is based on the specific heat of that phase and shared temperature. The source term, S_h is the volumetric heat source term. To simulate the heat transfer between the phases during the evaporation-condensation, modeling the heat source term is desired.

The rising vapor from the zeolite water mixture could be simulated using the VOF model with the

evaporation-condensation model. A two-phase approach was used with water vapor as the primary phase and liquid water as the secondary phase. The depth of the water was specified as 4 cm. The liquid volume was patched with the secondary phase volume fraction value of 1. Gravity was enabled to cover the natural gravitational drag for vapor condensing into fresh liquid water to drop out. A simple scheme was used to couple the pressure and velocity and second-order upwind scheme for spatial discretization of most of the governing terms. The default under-relaxation parameters were set for all the solution control panel.

Boundary conditions

An appropriate thermal boundary condition is necessary for any thermal system modeling to attain accurate predictions. The thermal energy absorbed by the zeolite-water mixture depends mainly on the solar incident radiation. In the current CFD simulations, isothermal boundary conditions are specified from the experimental results chosen from Figure 4. The experimental measured basin water-zeolite temperature, the inside air temperature, and glass cover at a certain time of day (i.e. at 13.00 h in all simulations run) were used as boundary conditions. The productivity of fresh water computed from CFD simulation results at a certain time of day are compared with the experimental results.

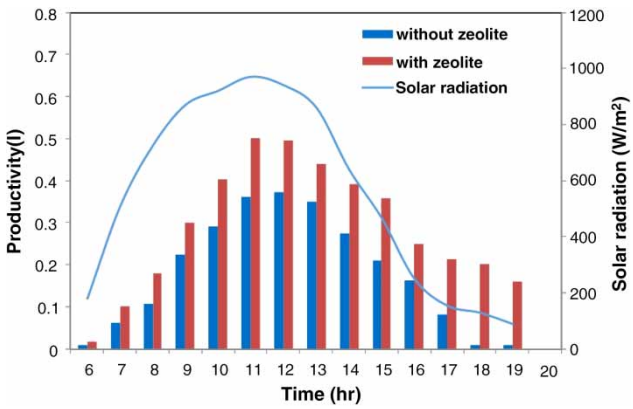

Figure 4 | Hourly variation of freshwater production for a solar still filled with and without zeolite at $\varphi = 0.05$.

RESULTS AND DISCUSSION

The experiments and CFD simulations were conducted to investigate the performance of the pyramid solar still in water production by introducing zeolite particles at various volume fractions. The system was operated continuously for several clear sky days in summer (month of June). The hourly solar radiation during one day of testing is shown in Figure 4. It shows also the variation of the solar radiation, which increases in the morning hours reaching its maximum values around midday and then decreases in the afternoon. The maximum value of solar incident radiation around midday was about 1,000 W/m^2.

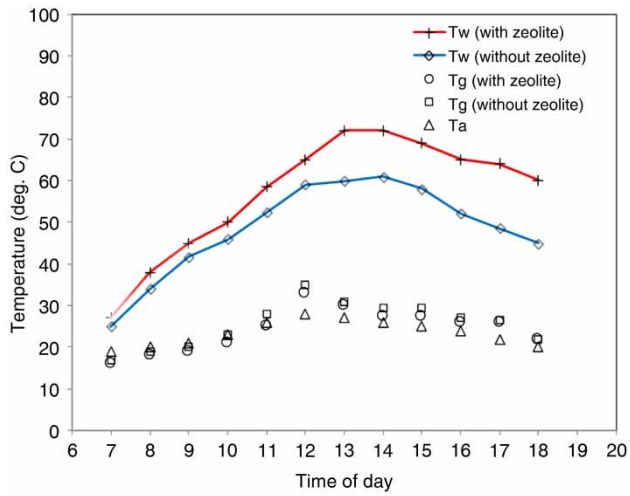

Figure 5 | Hourly variation of basin water temperature (T_w), glass cover temperature (T_g), and ambient temperature (T_a) during one day at $\varphi = 0.05$.

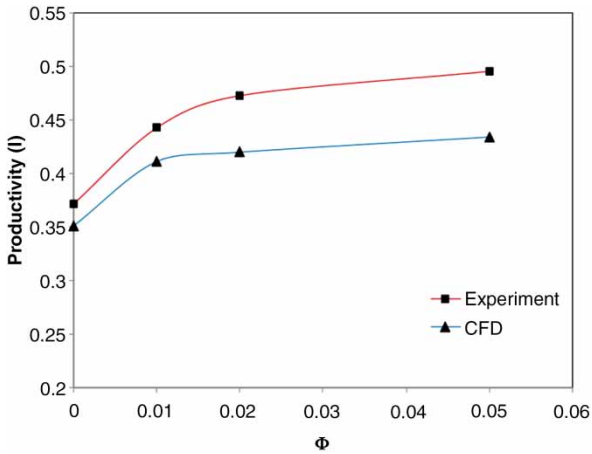

Figure 6 | Comparison of experimental and CFD simulation of productivity of solar still as a function of zeolite volume fraction at time 13.00 h.

The main parameter that has been examined in this study was the zeolite volume fraction in the solar still. The water depth (4 cm), insulation thickness (1 cm), salt concentration and ambient temperature remained invariant. The hourly variation of the experimental temperature of saline water, the glass cover, and the basin during one day of testing are depicted in Figure 5 for the solar still with and without zeolite particles.

As can be shown from Figure 5, the temperature values of the saline water, glass cover and the basin start to increase slowly in the morning hours and then reach their maximum values around midday and thereafter start to decrease in the evening. The temperature of the saline water in the solar still with zeolite particles seems to be higher than the temperature of the solar still without zeolite particles. The reason for this might be that the thermal absorption ability of the

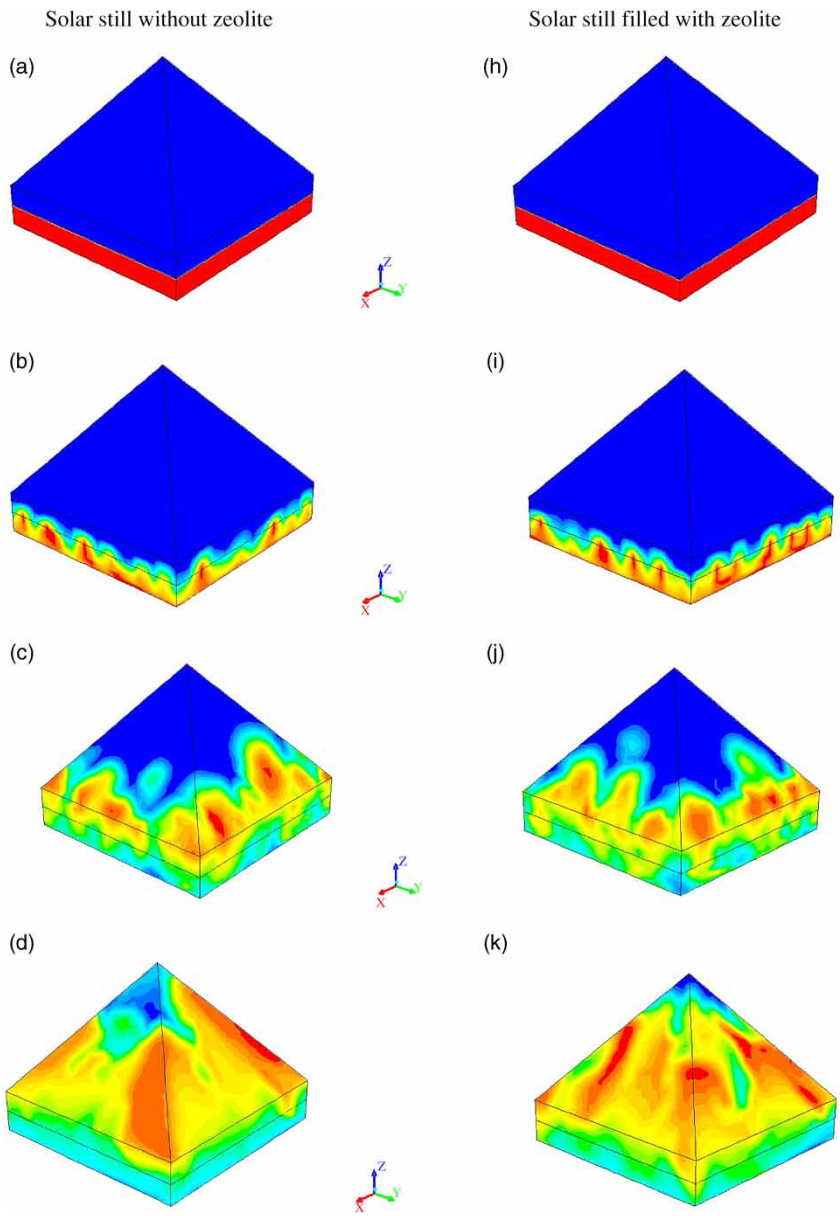

Figure 7 | Contours of water vapor fraction for still with (figure from (h) to (n)) and without (figure from (a) to (g)) zeolite particle load, ($\phi = 0.05$), time 13.00 h. *(Continued.)*

zeolite particles took in the basin increase, the zeolite temperature itself and also the basin surface temperature. This in turn increases the amount of vapor and thus the fresh water productivity. During the sunless hours, the zeolite particles act as a source of stored thermal energy that is stored and released before midday and after midday, respectively. The experimental and CFD results are presented to assess the effect of using zeolite particle loads on the yields of freshwater. The freshwater productivity rate (hourly variation of freshwater production) for the solar stills with and without zeolite particles is shown in Figure 4. It can be seen from Figure 4 that the yield of freshwater increases gradually to reach a maximum value around midday and then decreases in the afternoon, similar to the variation in incident solar radiation. It is also clear from Figure 4 that the productivity rate after midday is enhanced for the solar still with zeolite particles. Addition of zeolite particles in the basin increases the water temperature, and as a result, increases the evaporation rate. Zeolite of an average diameter 0.25 μm is used. At 18:00 h, the average volume of freshwater is found to be 0.01 L and 0.21 L, for the solar stills without and with zeolite particles, respectively. This is due to the presence of zeolite that increases the heat stored for water vaporization and thereafter condensation inside the solar still. Therefore, the increase in the freshwater yield during the sunless hours from 14.00 to 19.00 h is due to the zeolite particles

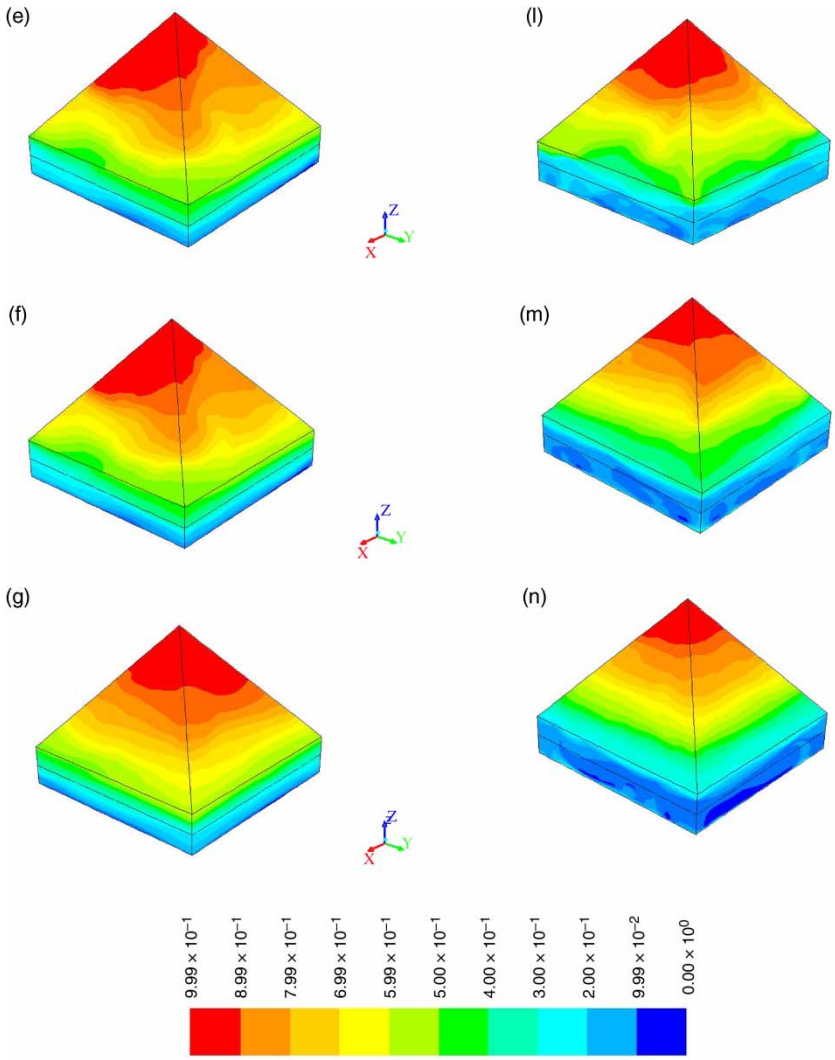

Figure 7 | Continued.

immersed inside the solar still. The comparative analyses of the experimental and CFD simulations of freshwater production rate for solar stills at various volume fractions are shown in Figure 6. It is noticeable that the water productivity increases with increasing zeolite volume fraction. The reason may be that when the mass of zeolite increases, the energy absorbed from the basin increases. This in turn enhances the evaporation rate as well as the mass productivity of the condensed water.

In order to assert the applicability of the developed evaporation-condensation CFD modeling to the VOF model, CFD simulation results of solar still productivity are compared with that of experiments. It can be noted from Figure 6 that the CFD proposed model and the experimental results for the case of the solar still without zeolite particles ($\phi = 0$) shows lower deviation than at higher zeolite particle volume fraction. It can be concluded that the CFD model has good agreement with the experiments at low particle volume fraction. The CFD model deviation from the experimental results increases with increasing zeolite particle volume fraction. The deviations of CFD from experimental results, for $\phi = 0.0$ and $\phi = 0.05$ are 0.05% and 12.3%, respectively. This can be attributed to the empirical formula that is used to calculate the effective thermal-physical properties that does not take temperature variation into account. Another reason may be that in reality there could be some sedimentation and agglomeration of the zeolite particles.

Figure 7 shows the contours of water-vapor volume fraction in the solar still with (Figure 7(h)–7(n)) and without zeolite particles (Figure 7(a)–7(h)). We have to mention here that the corresponding thermal boundary conditions (basin and glass temperature) implemented in the CFD model are obtained from Figure 5 at 13.00 h. At the beginning of the simulation the contours of the liquid fraction at the bottom of the solar still with a fixed water level are shown in Figure 7(a) and 7(h). As the temperature of the water inside the solar still increases, phase change starts and vapor is produced. The phase change can be noticed in Figure 7 from the increasing volume fraction of the secondary phase fluid (water vapor). The water vapor rises up as a result of a bouncy effect and is brought into contact with the low temperature glass surfaces at the top, the water vapor begins to condense and freshwater is produced. The fresh-water productivity as a result of condensation inside solar stills with and without zeolite particles is shown in Figure 7(f)–7(n). It can be noted that the rates of evaporation and thus condensation (fresh water) for stills with zeolite particles are enhanced, which can be seen from the increased volume fraction of the primary phase fluid (water liquid) in the basin outlet. The freshwater production was detected and the total water gained after 60 min was estimated

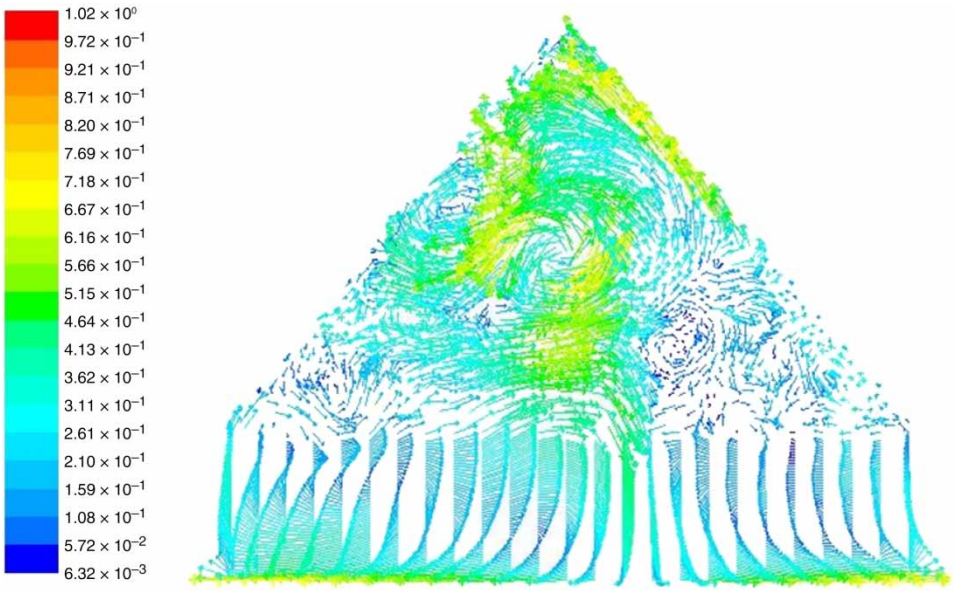

Figure 8 | Velocity vectors in the middle of the solar still without zeolite particles.

using CFD analysis. The freshwater production using CDF modeling at various zeolite volume fractions is depicted in Figure 6. Figure 8 shows the velocity vectors inside the solar still without zeolite in the middle plane. In general, the flow is generated by the moving of the water vapor upward (free convection). Primary and secondary vortices are formed inside the solar still due to the movement of water vapor that is released from the water surface.

CONCLUSIONS

The experimental and CFD modeling of a pyramid-shaped solar still was investigated. A 0.95 m^2 solar still was designed and constructed and its performance was evaluated under Jordanian weather conditions. The productivity of the solar still can be improved by adding zeolite particles. The obtained experimental results are compared with CFD simulation results. It was demonstrated that the present CFD results are in good agreement with the experimental results. This verifies the current adopted CFD model for freshwater prediction for such solar still configuration. Solar stills with zeolite provide an increase in water temperature especially after midday, as the zeolite acts as a heat source for the basin water.

REFERENCES

Abu-Arabi, M., Zurigat, Y. & Al-Hinaib, H. 2002 Modeling and performance analysis of a solar desalination unit with double-glass cover cooling. *Desalination* **143**, 173–182.

Djebedjian, B. & Abou Rayan, M. 2000 Theoretical investigation on the performance prediction of solar still. *Desalination* **128** (2), 139–145.

El-Sebaii, A. A., Aboul-Enein, S., Ramadan, M. R. I. & Khallaf, A. M. 2011 Thermal performance of an active single basin solar still (ASBS) coupled to shallow solar pond (SSP). *Desalination* **280**, 183–190.

Esfahani, J. A., Rahbar, N. & Lavvaf, M. 2011 Utilization of thermoelectric cooling in a portable active solar still - an experimental study on winter days. *Desalination* **269** (1–3), 198–205.

Hamdan, M. A., Musa, A. M. & Jubran, B. A. 1999 Performance of solar still under Jordanian climate. *Energy Convers. Manage.* **40**, 495–503.

Hirt, C. W. & Nichols, B. D. 1981 Volume of Fluid (VOF) method for the dynamics of free boundaries. *Journal of Computational Physics* **39** (1), 201–225.

Kabeel, A. E., Omara, Z. M. & Essa, F. A. 2014 Improving the performance of solar still by using nanofluids and providing vacuum. *Energy Conversion and Management* **8**, 268–274.

Khanafer, K., Vafai, K. & Lightstone, M. 2003 Buoyancy-driven heat transfer enhancement in a two dimensional enclosure utilizing nanofluids. *International Journal of Heat and Mass Transfer* **46** (19), 3639–3653.

Khanna, R. K., Rathore, R. S. & Sharma, C. 2008 Solar still an appropriate technology for potable water need of remote villages of desert state of India-Rajasthan. *Desalination* **220** (13), 645–653.

Kumar, S. & Tiwari, G. N. 1998 Optimization of collector and basin areas for a higher yield for active solar stills. *Desalination* **116** (1), 1–9.

Malik, M. A. S., Tiwari, G. N., Kumar, A. & Sodha, M. S. 1982 *Solar Distillation: A Practical Study of a Wide Range of Stills and Optimum Design, Construction and Performance*. Pergamon Press, New York.

Papanicolaou, E. & Belessiotis, V. 2005 Double-diffusive natural convection in an asymmetric trapezoidal enclosure: unsteady behavior in the laminar and the turbulent-flow regime. *International Journal of Heat and Mass Transfer* **48** (1), 191–209.

Rahbar, N. & Esfahani, J. A. 2013 Productivity estimation of a single-slope solar still: theoretical and numerical analysis. *Energy* **49** (1), 289–297.

Rheinländer, J. 1982 Numerical calculation of heat and mass transfer in solar stills. *Solar Energy* **28** (2), 173–179.

Taamneh, Y. & Al-Shyyab, A. 2016 Improvement of the performance of a solar still by utilizing the sorption thermal storage of natural zeolite. *Desalination and Water Treatment* **57** (57), 27450–27457. http://dx.doi.org/10.1080/19443994.2016.1176961.

Taamneh, Y. & Taamneh, M. 2012 Performance of pyramid-shaped solar still: experimental study. *Desalination* **291**, 65–68.

Tiwari, G. N., Mukherjee, K., Ashok, K. R. & Yadav, Y. P. 1986 Comparison of various designs of solar stills. *Desalination* **60** (2), 191–202.

Tiwari, G. N., Kupfermann, A. & Aggarwal, S. 1997 A new design for a double condensing chamber solar still. *Desalination* **114** (2), 153–164.

Tiwari, G. N., Shukla, S. K. & Singh, I. P. 2003 Computer modeling of passive/active solar stills by using inner glass temperature. *Desalination* **154** (2), 171–185.

Velmurugana, V. & Srithar, K. 2007 Solar stills integrated with a mini solar pond – analytical simulation and experimental validation. *Desalination* **216** (1–3), 232–241.

Voropoulos, K., Mathioulakis, E. & Belessiotis, V. 2001 Experimental investigation of a solar still coupled with solar collectors. *Desalination* **138** (1–3), 103–110.

First received 30 October 2015; accepted in revised form 17 May 2016. Available online 2 June 2016